DOI: 10.1093/jnci/djq257
Advance Access publication on July 21, 2010.

ARTICLE

GLI2-Mediated Melanoma Invasion and Metastasis

Vasileia-Ismini Alexaki, Delphine Javelaud, Leon C. L. Van Kempen, Khalid S. Mohammad, Sylviane Dennler, Flavie Luciani, Keith S. Hoek, Patricia Juàrez, James S. Goydos, Pierrick J. Fournier, Claire Sibon, Corine Bertolotto, Franck Verrecchia, Simon Saule, Veronique Delmas, Robert Ballotti, Lionel Larue, Philippe Saiag, Theresa A. Guise, Alain Mauviel

Manuscript received April 11, 2009; revised May 17, 2010; accepted June 1, 2010.

Correspondence to: Alain Mauviel, PhD, Curie Institute, INSERM U1021/CNRS UMR3347, University Center, Bldg 110, Rm 216, 91405 Orsay Cedex, France (e-mail: alain.mauviel@curie.fr).

Background The transforming growth factor-β (TGF-β) pathway, which has both tumor suppressor and pro-oncogenic activities, is often constitutively active in melanoma and is a marker of poor prognosis. Recently, we identified GLI2, a mediator of the hedgehog pathway, as a transcriptional target of TGF-β signaling.

Methods We used real-time reverse transcription–polymerase chain reaction (RT-PCR) and western blotting to determine GLI2 expression in human melanoma cell lines and subsequently classified them as GLI2high or as GLI2low according to their relative GLI2 mRNA and protein expression levels. GLI2 expression was reduced in a GLI2high cell line with lentiviral expression of short hairpin RNA targeting GLI2. We assessed the role of GLI2 in melanoma cell invasiveness in Matrigel assays. We measured secretion of matrix metalloproteinase (MMP)-2 and MMP-9 by gelatin zymography and expression of E-cadherin by western blotting and RT-PCR. The role of GLI2 in development of bone metastases was determined following intracardiac injection of melanoma cells in immunocompromised mice (n = 5–13). Human melanoma samples (n = 79) at various stages of disease progression were analyzed for GLI2 and E-cadherin expression by immunohistochemistry, in situ hybridization, or RT-PCR. All statistical tests were two-sided.

Results Among melanoma cell lines, increased GLI2 expression was associated with loss of E-cadherin expression and with increased capacity to invade Matrigel and to form bone metastases in mice (mean osteolytic tumor area: GLI2high vs GLI2low, 2.81 vs 0.93 mm^2, difference = 1.88 mm^2, 95% confidence interval [CI] = 1.16 to 2.60, $P < .001$). Reduction of GLI2 expression in melanoma cells that had expressed high levels of GLI2 substantially inhibited both basal and TGF-β-induced cell migration, invasion (mean number of Matrigel invading cells: shGLI2 vs shCtrl (control), 52.6 vs 100, difference = 47.4, 95% CI = 37.0 to 57.8, $P = .024$; for shGLI2 + TGF-β vs shCtrl + TGF-β, 31.0 vs 161.9, difference = −130.9, 95% CI = −96.2 to −165.5, $P = .002$), and MMP secretion in vitro and the development of experimental bone metastases in mice. Within human melanoma lesions, GLI2 expression was heterogeneous, associated with tumor regions in which E-cadherin was lost and increased in the most aggressive tumors.

Conclusion GLI2 was directly involved in driving melanoma invasion and metastasis in this preclinical study.

J Natl Cancer Inst 2010;102:1148–1159

Melanoma represents approximately 4% of human skin cancers, yet accounts for approximately 80% of deaths from cutaneous neoplasms (1). Although progress has been made in understanding the genetics of the molecular events underlying melanoma oncogenesis (2–4), the clinical challenge remains enormous. A genetic hallmark of melanoma is the presence of activating mutations in the oncogenes *BRAF* and *NRAS*, which are present in 70% and 15% of melanomas, respectively, and lead to constitutive activation of mitogen-activated protein kinase pathway signaling (3,5). However, molecules that inhibit mitogen-activated protein kinase pathway–associated kinases, like BRAF and MEK, have shown only limited efficacy in the treatment of metastatic melanoma (6). Thus, a deeper understanding of the cross talk between signaling networks and the complexity of melanoma progression should lead to more effective therapy.

Hedgehog (HH) signaling is controlled at the cell surface by two transmembrane proteins, the tumor suppressor Patched-1 (PTCH1), which acts as a HH receptor, and the oncoprotein Smoothened (SMO). In the absence of HH, PTCH1 maintains SMO in an inactive state. In the presence of any of the three HH ligands (Sonic, Indian, or Desert HH), inhibition of SMO by PTCH1 is alleviated and a signal is transduced that leads to the nuclear translocation and activation of GLI family transcription factors (7,8). GLIs are often overexpressed in cancers and contribute to the progression of a variety of neoplasms via regulation of cell cycle progression and apoptosis (9,10). One recent study (11)

suggested that the HH pathway may play a role in melanoma progression based on pharmacological inhibition of HH signaling in genetic mouse models of melanoma.

Transforming growth factor-β (TGF-β) is a potent inhibitor of normal epithelial cell proliferation. However, it is secreted in abundance by tumor cells and exerts pro-oncogenic activities in later stages of tumor progression (12–14). Members of the TGF-β superfamily signal via heteromeric serine/threonine kinase transmembrane receptor complexes that, on ligand binding, phosphorylate SMAD family proteins that mediate signaling from the cell membrane to the nucleus (15,16). In vivo, malignant melanomas secrete high amounts of TGF-β, and increased circulating plasma concentrations of TGF-β are associated with the advancing stage of the tumor (17,18). TGF-β also exerts paracrine effects on angiogenesis and immune surveillance, thereby promoting tumor growth and survival (19). Autocrine TGF-β signaling and SMAD-dependent transcriptional responses directly exacerbate melanoma cell tumorigenicity and metastasis (20–22).

Recently, we determined that the gene for GLI2, which is the most transcriptionally active of the GLI proteins, was directly induced by TGF-β and SMAD signaling (23). Furthermore, the GLI2 protein mediates the induction of GLI1 expression in response to TGF-β, independent of HH signaling (23).

In this report, we have analyzed the specific role played by GLI2 in human melanoma. We used a combination of in vitro and in vivo experimental approaches to determine whether GLI2 expression is associated with melanoma cell invasion, matrix metalloproteinase (MMP) secretion, expression of E-cadherin, and metastasis to bone. Reduction of GLI2 expression with specific short hairpin RNA (shRNA) vectors was used to directly address the functionality of GLI2 in these experimental settings. To gain insight into the pathophysiological relevance of our findings in melanoma, expression of GLI2, together with that of E-cadherin, was determined in human melanoma tumors.

CONTEXT AND CAVEATS

Prior knowledge

The gene for hedgehog pathway component GLI2 was reported to be induced by transforming growth factor-β signaling, which promotes melanoma tumorigencitiy, but a role for GLI2 in melanoma invasion and metastasis had not been tested.

Study design

Melanoma cell lines that expressed high or low levels of GLI2 (GLI2high vs GLI2low) or that expressed shRNA to GLI2 or constitutively active GLI2 were compared in Matrigel invasion assays and in assays of bone metastasis after intracardiac injection of immunocompromised mice. Levels of GLI2 expression were also examined in staged human melanoma tissue specimens.

Contribution

Elevated GLI2 expression was associated with greater invasiveness of melanoma cells in vitro and with increased number and size of osteolytic metastases in mice. Overall, GLI2 expression was increased in more aggressive tumors.

Implications

GLI2 may play a role in melanoma invasion and metastasis.

Limitations

Most experiments were done with melanoma cell lines in an in vitro invasion assay or in an immunocompromised mouse model of bone metastasis, whereas in immunocompetent humans, melanoma cells would most likely metastasize to lung, soft tissue, and brain. Evaluation of GLI2 in clinical specimens was limited by the number of specimens available and the lack of a good antibody for immunohistochemistry.

From the Editors

Materials and Methods

Cell Cultures and Reagents

Human melanoma cell lines that were derived from tumor biopsies from patients with either primary (WM793, 888mel, Dauv1, and WM983A) or metastatic (WM983B [same patient as WM983A], WM852, 501mel, FO-1, and SK28) melanoma lesions were grown in RPMI 1640 (Invitrogen, Carlsbad, CA) supplemented with 10% fetal calf serum (FCS) and antibiotics. 1205Lu melanoma cells were derived from WM793 cells by serial passage through athymic mice and selection of cells metastatic to the lungs. WM cell lines were a gift from Meenhard Herlyn (Wistar Institute, Philadelphia, PA). FO-1 cells were a gift from Renato Baserga (Thomas Jefferson University, Philadelphia, PA). 888mel and SK28 cell lines were purchased from American Type Culture Collection (Manassas, VA). Dauv1 cells were a gift from Benoit van den Eynde (Ludwig Institute for Cancer Research, Brussels, Belgium). All cell lines in this panel carry an activating mutation of the *BRAF* gene, except for WM852 cells, which carry an activating mutation of *NRAS* (24). Additional details may be found in previous publications (20,22,25–27). Normal human foreskin epidermal melanocytes (passages 5–8) were purchased from PromoCell GmbH (Heidelberg, Germany). All melanocyte cell lines were verified to express melanocyte-microphthalmia-associated transcription factor (M-MITF), a marker of the melanocytic lineage, at detectable levels by quantitative reverse transcription–polymerase chain reaction (RT-PCR). Lentiviral particles expressing GLI2 shRNAs were purchased from Sigma-Aldrich (St Louis, MO). TGF-β_1 was purchased from R&D Systems, Inc (Minneapolis, MN). Expression vectors carrying dominant-negative and constitutively active versions of mouse *GLI2* and the GLI-specific reporter plasmid $(GLI\text{-}BS)_8$-luc were gifts from H. Sasaki (Osaka University) and have been described previously (28,29). pRL-TK was from Promega (Madison, WI).

RNA Extraction and Gene Expression Analysis

Total RNA was isolated from cell cultures using an RNeasy kit (Qiagen GmbH, Hilden, Germany). Genomic DNA contamination was eliminated by DNase I treatment. One microgram of RNA was reverse transcribed using the Thermoscript kit (Invitrogen). The resulting cDNAs were then processed for either semiquantitative or real-time RT-PCR using either ethidium bromide staining of electrophoretically separated amplimers or SYBR Green technology (Applied Biosystems, Foster City, CA). In the latter case, reactions were carried out in a 7300 Real-Time PCR System (Applied Biosystems) for 40 cycles (95°C for

15 seconds and 60°C for 1 minute) after an initial 10-minute incubation at 95°C. Data were analyzed using Applied Biosystems Sequence Detection Software (version 1.2.1) and normalized to cyclophilin A (PPIA) or glyceraldehyde-3-phosphate dehydrogenase (GAPDH) expression. Five independent experiments were performed to validate gene expression data in each cell line. Primer sequences for multiplex semiquantitative RT-PCR and for real-time RT-PCR are provided in Supplementary Tables 1 and 2, respectively (available online).

Western Blotting

Protein extraction and western blotting were performed in three independent experiments as previously described (22). Goat polyclonal anti-GLI2 (sc-20291, 1:200 dilution); rabbit polyclonal anti-E-cadherin (sc-7870, 1:500 dilution); and secondary donkey anti-mouse, anti-goat, and anti-rabbit horseradish peroxidase–conjugated antibodies were from Santa Cruz Biotechnology, Inc (Santa Cruz, CA). Mouse monoclonal anti-GAPDH (ab8245, 1:5000 dilution) was from Abcam (Cambridge, MA), and anti-β-actin (A4700, 1:1000 dilution) was from Sigma-Aldrich.

Stable GLI2 Silencing in 1205Lu Human Melanoma Cells

Subconfluent 1205Lu cells were infected with lentiviruses that expressed either control, nontargeting, shRNA (shCtrl; Sigma-Aldrich SHC002V) or shRNA targeting GLI2 (Sigma-Aldrich SHVRS clone ID TRCN0000033329 and TRCN0000033330) at a multiplicity of 8 plaque-forming units per cell in presence of 8 μg/mL hexadimethrine bromide. Stably transduced cell populations were selected with puromycin (2 μg/mL). Efficient and stable reduction of GLI2 mRNA expression over time was verified by real-time RT-PCR after each passage and before experiments.

Stable Transfections

Truncated forms of mouse *GLI2* that expressed GLI2 proteins with deletions of amino acids 1184–1544 (GLI2-ΔC2) or 1–279 (GLI2-ΔN2) were used as dominant-negative and constitutively active GLI2 mutants, respectively (29). SK28 and 1205Lu melanoma cells were transfected at approximately 70%–80% confluence with 10 μg of either the empty expression vector (ctrl) or the same vector carrying constitutively active GLI2-ΔN2 or dominant-negative GLI2-ΔC2 (29) per 100-mm-diameter culture dish using the polycationic compound Fugene (Roche Diagnostics, Indianapolis, IN) in fresh medium containing 1% FCS. Three days later, G418 (Sigma-Aldrich, 0.7 mg/mL) was added to the culture medium. Selection of stable clones occurred within a 3-week period. Semiquantitative RT-PCR was used to verify the expression of the transfected gene constructs.

Transient Cell Transfections and Reporter Assays

SK28 melanoma cells were seeded in 24-well plates and cotransfected with $(GLI\text{-}BS)_8$-luc (28) and pRL-TK as a control for transfection efficiency (Promega). Cells were transfected at approximately 70%–80% confluence using the polycationic compound Fugene (Roche Diagnostics) in fresh medium containing 1% FCS. Following a 16-hour incubation, cells were rinsed twice with phosphate-buffered saline (PBS) and lysed in passive lysis buffer (Promega). Luciferase activities were determined with a Dual-Glo luciferase assay kit according to the manufacturer's protocol (Promega). In general, three independent experiments were performed using triplicate samples, but the number varied among experiments and is detailed in the corresponding figure legends.

Matrigel Invasion Assays

Tissue culture Transwell inserts (8 μm pore size; Falcon, Franklin Lakes, NJ) were coated for 3 hours with 10 μg of growth factor–reduced Matrigel (Biocoat; BD Biosciences, San Jose, CA) in 100 μL of PBS at 37°C. After air-drying the chambers for 16 hours, the Matrigel barrier was reconstituted with 100 μL Dulbecco's minimal essential medium for 24 hours at 37°C. The chambers were then placed into 24-well dishes containing 750 μL of RPMI medium supplemented with 0.1% FCS. 5×10^4 melanoma cells (1205Lu, WM793, WM852, Dauv1, WM983A, WM983B, SK28, 501mel, and 888mel) were added to the upper well of each chamber in 500 μL of serum-free RPMI medium. After a 24-hour incubation period, the number of invading cells was counted by bright field microscopy at ×200 in six random fields. Additional details of the procedure may be found in Javelaud et al. (21). Experiments were performed four times using duplicate samples.

Gelatin Zymography

The presence of MMP-2 and MMP-9 in serum-free conditioned media was analyzed by zymography in 10% sodium dodecyl sulfate–polyacrylamide gels containing 1 mg/mL gelatin (Sigma-Aldrich). After removal of sodium dodecyl sulfate with Triton X-100, neutral protease activity was revealed by incubation of the gels for 48 hours at 37°C in 0.1 M Tris–HCl buffer (pH 7.4) containing 10 mM $CaCl_2$, followed by staining in 0.5% Coomassie blue in an aqueous solution containing 30% isopropanol and 10% acetic acid and destaining in 30% isopropanol and 10% acetic acid (30). Three independent experiments were performed.

Wound Closure Assays

For scratch wound assays, freshly confluent monolayers of shCtrl and shGLI2-transfected 1205Lu cells were wounded by manually scraping off cells with a sterile pipette tip. Following wounding of the monolayers, wound sizes were verified to ensure that they were all the same width (approximately 0.8 mm). The cell culture medium was then replaced with fresh RPMI containing 4 μg/mL mitomycin C (Sigma-Aldrich), and wound closure was monitored over a 48-hour period with a phase contrast microscope at ×200 magnification. Experiments were repeated three times.

Experimental Bone Metastasis in Mice

The protocols for bone metastasis experiments in athymic female nude mice were approved by the Institutional Animal Care and Use Committee at the University of Virginia in Charlottesville and were in accordance with the National Institutes of Health Guide for the Care and Use of Laboratory Animals. Harlan-Sprague-Dawley athymic nude-Foxn Nu mice (*nu/nu*, n = 72) were purchased from Harlan (Indianapolis, IN). In brief, following anesthesia of each mouse by intraperitoneal injection with a mixture of 30% ketamine and 20% xylazine in 0.9% NaCl (7 mg/100 g body weight), the left cardiac ventricle was punctured percutaneously using a 26-gauge needle attached to a 1-mL syringe containing suspended tumor

cells. Visualization of bright red blood entering the hub of the needle in a pulsatile fashion indicated a correct position in the left cardiac ventricle. Tumor cells (10^5 in 0.1 mL of PBS) were inoculated slowly over 1 minute. Mice were followed by radiography for the development of bone lesions throughout the experiments. Images were saved, and lesion areas were measured and analyzed using MetaMorph software (Molecular Devices, Downingtown, PA). Briefly, the images were calibrated, and the edges of the translucent area that represents area of bone loss were identified and traced with a computer mouse pointer, and the area was measured in squared millimeter units. Details of the experimental procedures may be found in several past publications (22,31–33). Mice bearing human tumor xenografts were carefully monitored for established signs of distress and discomfort including development of cachexia (as defined by loss of 20% of original body weight) and inability of the mouse to move and reach for the food source and were humanely killed when these were confirmed.

Immunohistochemistry and In Situ Hybridization on Human Tissues

Formaldehyde-fixed and paraffin-embedded melanomas (n = 20) from adult patients were obtained from the pathology archives of the Radboud University Nijmegen Medical Centre. All specimens were reevaluated by an expert pathologist. Tissues were obtained according to local ethical guidelines and approved by the local regulatory committee. Paraffin-embedded 4-μm sections were dewaxed and rehydrated through graded alcohol baths. After an antigen retrieval step with Tris-buffered EDTA (1 mM, pH 9.0, for 10 minutes at 95°C), tissue paraffin sections were preincubated with 20% normal horse serum and subsequently incubated with a mouse monoclonal antibody directed against E-cadherin (Neomarkers, clone SPM471, 1:300 dilution) in PBS containing 1% bovine serum albumin overnight at 4°C. As a secondary reagent, a horseradish peroxidase–conjugated goat anti-mouse antibody from the Powervision system (Immunovision Labs, Brisbane, CA) was used at a 1:2 dilution. Diaminobenzidine served as a chromogen. Counterstaining was performed with hematoxylin.

For in situ hybridization, a 340-bp human *GLI2* cDNA fragment was generated by RT-PCR. Briefly, total RNA isolated from 1205Lu melanoma cells was isolated with Trizol (Invitrogen) according to the manufacturer's protocol, and 1 μg was reverse transcribed at 42°C for 1 hour using SuperScript II (Invitrogen) and oligo dT primers. First strand 5′ cDNA samples were amplified using oligonucleotide primer pairs (5′-AGTTTGTTCT CGGGTGCTCTG-3′ and 5′-ACATCTGTCATCTGAAGC GGC-3′) based on the reported sequence of human *GLI2* (GenBank accession number NM005270). Amplification consisted of preincubation at 95°C for 5 minutes before adding Taq polymerase followed by 30 cycles at 95°C for 1 minute, 60°C for 30 seconds, and 72°C for 30 seconds. A PCR product of the predicted size was cloned into the pGEM-T easy vector (Promega), and the sequence was verified. The plasmid was linearized by digestion with *Pst*I or *Sph*I. Antisense and sense digoxygenin-labeled rUTP riboprobes were synthesized using T7 and SP6 RNA polymerase, respectively, according to standard procedures. The in situ hybridization procedure was performed as described earlier (34) using tissue sections adjacent to those used for anti-E-cadherin or hematoxylin and eosin staining.

Tissue Harvesting and Total RNA Isolation

Tumor samples were obtained through the Tissue Retrieval Service of the Cancer Institute of New Jersey, following ethical committee guidelines of the University of Medicine and Dentistry of New Jersey (UMDNJ)-Robert Wood Johnson Medical School Institutional Review Board (n = 42), and from the tissue bank at Hôpital Ambroise Paré under the supervision of the local ethical committee (Comité de Protection des Personnes IDF8) (n = 17). Tissue samples were collected such that no patient-identifiable information was included with the specimens, but tumor location and stage were recorded. Details have been described previously (35). Tumor specimens from both locations had been flash frozen in liquid nitrogen within 5 minutes of resection and stored until RNA extraction. Total RNA was isolated from samples using a standard, spin column–based kit (RNeasy; Qiagen) and reverse transcribed for subsequent PCR analysis.

Statistical Analyses

For Matrigel invasion and gene expression in human tumor samples, we used the *t* test to calculate 95% confidence intervals (CIs) on differences between means and the Mann–Whitney test to obtain the *P* value. For data related to experimental bone metastasis in mice, differences in osteolytic lesion areas between groups were determined by two-way analysis of variance with Bonferroni posttests (GraphPad Prism). All statistical tests were two-sided. All results were expressed as means with 95% confidence intervals, and $P < .05$ was considered to be statistically significant.

Results

GLI2 Expression and Invasive Potential of Human Melanoma Cell Lines

We first determined the expression of the main HH pathway components in a panel of 10 human melanoma cell lines by semiquantitative RT-PCR. GLI2 expression was highly variable: Dauv1, WM852, 1205Lu, and WM793 cells expressed high levels of GLI2 mRNA (Figure 1, A, lanes 2, 6, 9, and 10), whereas in 888mel, 501mel, and FO-1 cells (lanes 3–5), GLI2 mRNA was barely detectable under the same PCR conditions. SK28, WM983B, and WM983A cell lines (lanes 1, 7, and 8) expressed GLI2 mRNA at intermediate levels, similar to those found in normal human melanocytes (lane 11). Expression of PTCH1, which was previously identified as a GLI2 transcriptional target (36), was increased in all but one cell line, WM852, among those cell lines that expressed GLI2 mRNA at high levels, and expression of GLI1, another known GLI2 target (37), was also elevated in all cell lines that expressed high levels of GLI2 mRNA except Dauv1 cells. Sonic hedgehog mRNA was undetectable in all melanoma cell lines except 501mel, whereas it was readily detected under the same PCR conditions in human pancreatic adenocarcinoma cell lines (data not shown). Expression of SMO and GLI3, at the mRNA level, was similar among all melanoma cell lines. Quantitative RT-PCR confirmed the results of multiplex semiquantitative RT-PCR and determined that GLI2 mRNA expression in Dauv1,

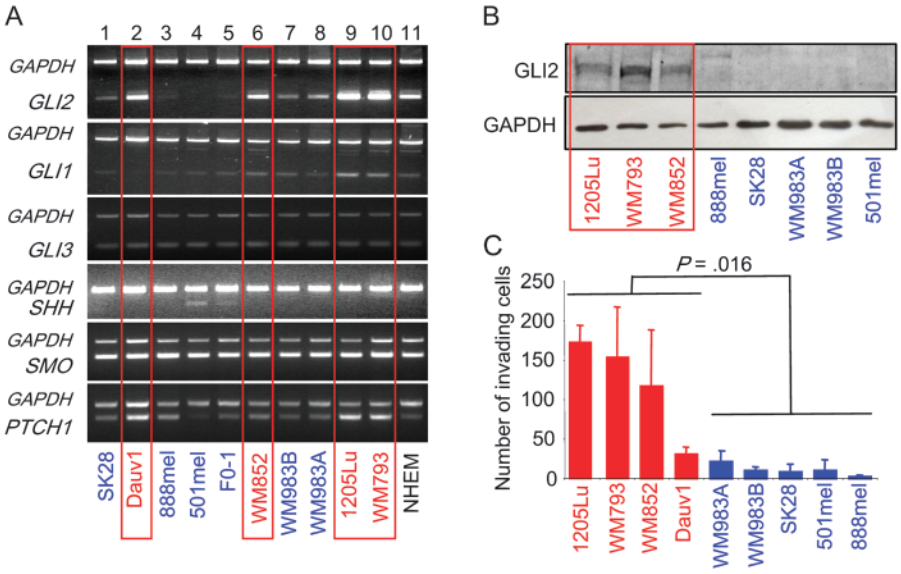

Figure 1. Expression of Sonic Hedgehog (SHH) pathway components in a panel of human melanoma cell lines and relationship between GLI2 levels and Matrigel invasion. Cell lines expressing high levels of GLI2 (GLI2high) are shown in **red**, and cell lines expressing low levels of GLI2 (GLI2low) are shown in **blue**. **A**) Semiquantitative multiplex reverse transcription–polymerase chain reaction (RT-PCR). GLI1, GLI3, GLI2, SHH, Smoothened (SMO), and Patched1 (PTCH1) mRNA expression was measured in 10 human melanoma cell lines (lanes 1–10) and normal human epidermal melanocytes (NHEM, lane 11) in culture. Expression of the glyceraldehyde-3-phosphate dehydrogenase gene, *GAPDH*, was examined as a control in the same RT-PCR reaction as each gene of interest. **B**) Western blot analysis. GLI2 protein levels were determined in various melanoma cell lines using 100 μg protein per lane. Determination of GAPDH levels served as a loading control. **C**) Matrigel invasion assay. Melanoma cells (5×10^4) were added to the upper well of each Matrigel invasion chamber in serum-free RPMI medium. The number of invading cells was counted 24 hours later using bright field microscopy at ×200 in six random fields. Experiments were performed four times using duplicate samples for each cell line. Statistical significance was calculated using the Mann–Whitney test. **Error bars** = 95% confidence intervals. GLI2high vs GLI2low groups: $P = .016$. All statistical tests were two-sided.

WM852, 1205Lu, and WM793 cell lines was about 200-fold higher than that in 888mel, 501mel, or FO-1 cells, and 15-fold higher than that in SK28, WM983A, and WM983B cells (data not shown).

Western blot analysis showed that GLI2 protein was abundant in WM852, 1205Lu, and WM793 cells (Figure 1, B) but undetectable in 888mel, SK28, WM983A, WM983B, and 501mel cells. Also, indirect immunofluorescence staining of GLI2 protein in 1205Lu, WM793, and WM852 cell cultures indicated that the GLI2 protein was almost exclusively localized in cell nuclei (data not shown).

Together, these results indicated that GLI2 mRNA expression is highly variable in human melanoma cell lines, with GLI2 protein content usually in accordance with steady-state levels of GLI2 mRNA. We subsequently referred to the group of cell lines that exhibited both high GLI2 RNA and protein levels (ie, 1205Lu, WM793, and WM852 plus Dauv1 cells) as "GLI2high" cells, whereas all other cell lines that we used (ie, WM983A, WM983B, SK28, 501mel, 888mel, and FO-1) were considered to be "GLI2low." GLI2 protein levels were never checked in Dauv1 cells.

We found no obvious link between the levels of GLI2 expression and melanoma cell growth in vitro when comparing Dauv1, 888mel, 501mel, FO-1, WM852, WM983B, WM983A, 1205Lu, and WM793 cell lines (data not shown). Likewise, GLI2high (1205Lu and Dauv1) and GLI2low (SK28, 888mel, and 501mel) melanoma cells lines could not be differentiated based on their capacity to form subcutaneous tumors in a subcutaneous xenograft growth assay in nude mice (data not shown).

Next, we compared the invasive capacity of melanoma cell lines in a Matrigel invasion assay. GLI2high cell lines (1205Lu, WM793, WM852, and, to a lesser extent, Dauv1) were all more invasive than GLI2low cell lines (Figure 1, C), suggesting a more aggressive phenotype.

Gelatin zymography identified markedly higher levels of MMP-2 secreted by the GLI2high cell lines (1205Lu, WM852, and, to a lesser extent, Dauv1), as compared with the GLI2low cell lines (WM983A, WM983B, SK28, 501mel, and 888mel; data not shown). MMP-2 is an extracellular matrix–degrading enzyme that is often used by cancer cells to invade basement membranes and progress toward a metastatic state (38).

Modulation of the Invasive Potential of Melanoma Cells by Altering GLI2 Function

To ascertain a causal relationship between GLI2 expression levels and melanoma cell aggressiveness, we transduced 1205Lu cells with a lentiviral vector carrying GLI2-specific shRNA to establish stable reduction of GLI2 protein expression or with a vector that expressed a control shRNA. GLI2 silencing resulted in approximately 85% reduction in GLI2 protein expression (Figure 2, A), a marked (approximately 75%) reduction in MMP-2 secretion (Figure 2, B) and a 50%–70% inhibition of the invasive capacity of 1205Lu cells in Matrigel (mean invasiveness for shGLI2 vs shCtrl, 52.6 vs 100 cells per six random microscopic fields, difference = 47.4, 95% CI = 37.0 to 57.8, $P = .024$) (Figure 2, C). Notably, reduction of GLI2 protein levels also abrogated the stimulatory effect of TGF-β on MMP-2 and MMP-9 secretion (Figure 2, B) and on Matrigel invasion (in the presence of TGF-β, mean invasiveness for shGLI2 vs shCtrl, 31.0 cells per six random microscopic fields vs 161.9 cells per six fields, difference = −130.9, 95% CI = 96.2 to 165.5, $P = .002$) (Figure 2, C). Furthermore, reduction of GLI2 protein levels strongly impaired cell motility, as visualized by the delayed closure of the gaps generated in cultured 1205Lu cell monolayers in the scratch wound assay (Figure 2, D), and by 85% inhibition of 1205Lu cell migration in a Transwell migration assay (data not shown). Similar results were obtained when GLI2-dependent transcription was altered in 1205Lu melanoma cells by means of stable expression of a dominant-negative mutant form of GLI2, GLI2-ΔC2 (29) (data not shown).

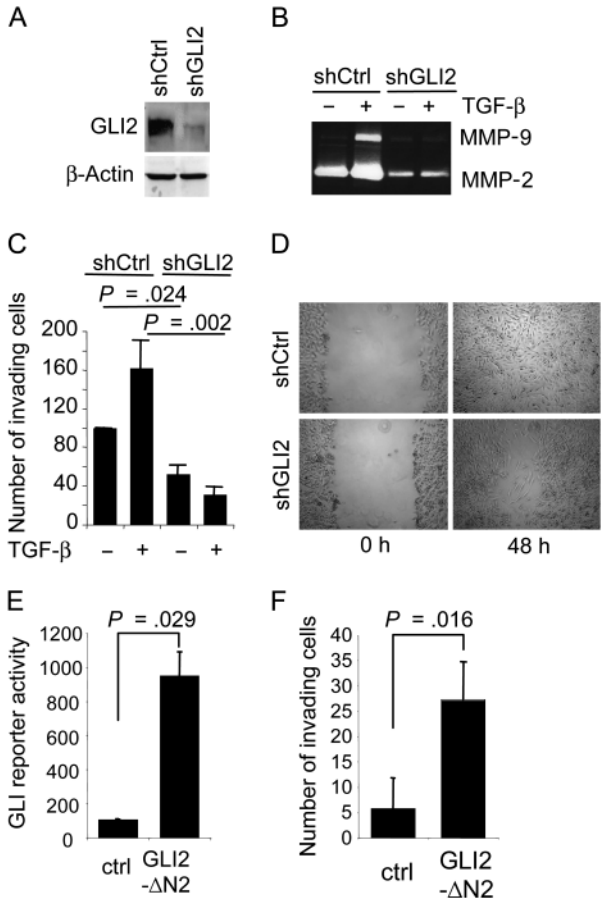

Figure 2. A role for GLI2 in melanoma cell migration and invasion. **A**) GLI2 silencing. GLI2 protein expression was silenced in 1205Lu human melanoma cells by infection with lentiviral particles carrying a short hairpin RNA (shRNA) against GLI2 (shGLI2). A nontargeting shRNA (shCtrl) was used as control. Relative GLI2 protein levels were measured by western blotting, and blots were reprobed with antibody to β-actin as an internal control. **B**) Matrix metalloproteinase (MMP)-2 and MMP-9 secretion by 1205Lu cells expressing shGLI2 or control shRNAs. Cells were cultivated 72 hours in serum-free medium in the absence or presence of 10 ng/mL transforming growth factor-β (TGF-β), conditioned medium was collected and subjected to electrophoresis, and MMP activity was visualized by gelatin zymography. The experiment was repeated three times, and a representative experiment is shown. **C**) Matrigel invasion assay. After stable transfection with control shRNA (shCtrl) or shGLI2, 1205Lu melanoma cells were incubated in the absence or presence of 10 ng/mL TGF-β. Then, 5×10^4 cells were added to the upper well of each Matrigel invasion chamber in serum-free RPMI medium with or without 10 ng/mL TGF-β. The number of invading cells was counted 24 hours later using bright field microscopy at ×200 in six random fields. Results are expressed as the mean of two independent experiments, each performed in duplicate. **D**) Wound closure assays. Confluent monolayers of shCtrl and shGLI2 1205Lu melanoma cells were wounded by a scratch with a pipette tip. Culture medium was replaced with fresh medium containing mitomycin (4 μg/mL) to prevent cell proliferation. Wound closure was monitored by phase contrast microscopy. A representative photomicrograph at ×200 magnification for each condition is shown. Photos were taken immediately (0 hours) or 48 hours after wounding. Experiments were repeated three times with similar results. **E**) GLI-dependent transcription. SK28 human melanoma cells were stably transfected with either an expression vector carrying the gene for the constitutively active mutant, GLI2-ΔN2, or the empty vector (ctrl). GLI-dependent transcription was measured by transient transfection of these cells with the GLI reporter construct $(GLI\text{-}BS)_8$-luc and measurement of the activity of the luciferase reporter. Results, expressed as relative luciferase activity, are the mean of two independent experiments, each performed with duplicate samples. **F**) Matrigel invasion assays of ctrl- and GLI2-ΔN2–transfected SK28 melanoma cells. The cells described in (**E**) were treated as described in (**C**). The number of invading cells was counted 24 hours later using bright field microscopy at ×200 in six random fields. Results are expressed as the mean of three independent experiments, each performed in duplicate. Statistical analysis was performed using the Mann–Whitney test. **Error bars** are 95% confidence intervals. All statistical tests were two-sided.

Inversely, stable expression of a constitutively active form of GLI2, GLI2-ΔN2, in the GLI2low SK28 melanoma cell line effectively enhanced GLI-dependent transcription (Figure 2, E) and dramatically increased the capacity of SK28 cells to invade Matrigel (mean invasiveness for GLI2-ΔN2–expressing SK28 cells vs control SK28 cells, 28.5 vs eight cells per six random microscopic fields, difference = −20.5, 95% CI = −36.4 to −4.60, $P = .057$) (Figure 2, F). Taken together, these experiments establish a direct role for GLI2 in driving the invasive potential of melanoma cells.

GLI2 Expression Levels in Melanoma Cells and Occurrence of Experimental Bone Metastasis in Mice

1205Lu cells rapidly metastasize to bone in a mouse model in which tumor cells are inoculated into the left cardiac ventricle of nude mice (22). This model addresses the process of metastasis from the entry of tumor cells into the arterial circulation to the establishment of bone metastasis and tumor–bone interactions. In a first set of experiments, two GLI2high cell lines (1205Lu and WM852) and three GLI2low cell lines (888mel, SK28, and 501mel) were compared for their capacity to form bone metastases. The two GLI2high cell lines caused osteolytic bone metastases in 100% of mice (seven of seven 1205Lu and eight of eight WM852 mice) 4 weeks after intracardiac inoculation. By contrast, only two of the five (40%), five of the eight (62.5%), and five of the seven (71.5%) mice inoculated with GLI2low cell lines SK28, 888mel, and 501mel, respectively, developed bone metastases (Figure 3, A). Notably, all mice bearing GLI2low melanoma cell lines had statistically significantly longer survival than mice bearing GLI2high melanoma cell lines (mean for SK28 = 35.6 days, 95% CI = 31.7 to 39.5; mean for 888mel = 44.4 days, 95% CI = 38.2 to 50.6; mean for 501mel = 35.6 days, 95% CI = 28.0 to 43.2; mean for 1205Lu = 29.6 days, 95% CI = 28.8 to 30.3; mean for WM852 = 29.8 days, 95% CI = 29.2 to 30.3; mean survival for all GLI2high cell lines [1205Lu + WM852] = 29.7 days, mean survival for all GLI2low cell lines [888mel + SK28 + 501mel] = 39.1 days, difference = 9.4 days, 95% CI = 5.2 to 13.6, $P < .001$). Individual differences in survival were as follows: SK28 vs 1205Lu = 6 days, 95% CI = 3.3 to 8.7, $P = .01$; SK28 vs WM852 = 5.9 days, 95% CI = 3.4 to 8.3, $P = .01$; 888mel vs 1205Lu = 14.8 days, 95% CI = 8.7 to 20.9, $P = .001$; 888mel vs WM852 = 14.6 days, 95% CI = 8.9 to 20.3, $P = .001$; 501mel vs 1205Lu = 6 days, 95% CI = −0.8 to 12.8, $P = .07$; 501mel vs WM852 = 5.8 days, 95% CI = −0.4 to 12.1, $P = .12$) (Figure 3, B). Likewise, at the 4-week time point, the two-dimensional area on x-rays that was occupied by the osteolytic lesions was substantially lower in mice that had been inoculated with GLI2low cells as compared with that in mice that had been inoculated with GLI2high cells (mean osteolytic tumor area for all GLI2high [1205Lu + WM852] vs all GLI2low [SK28 + 888mel +

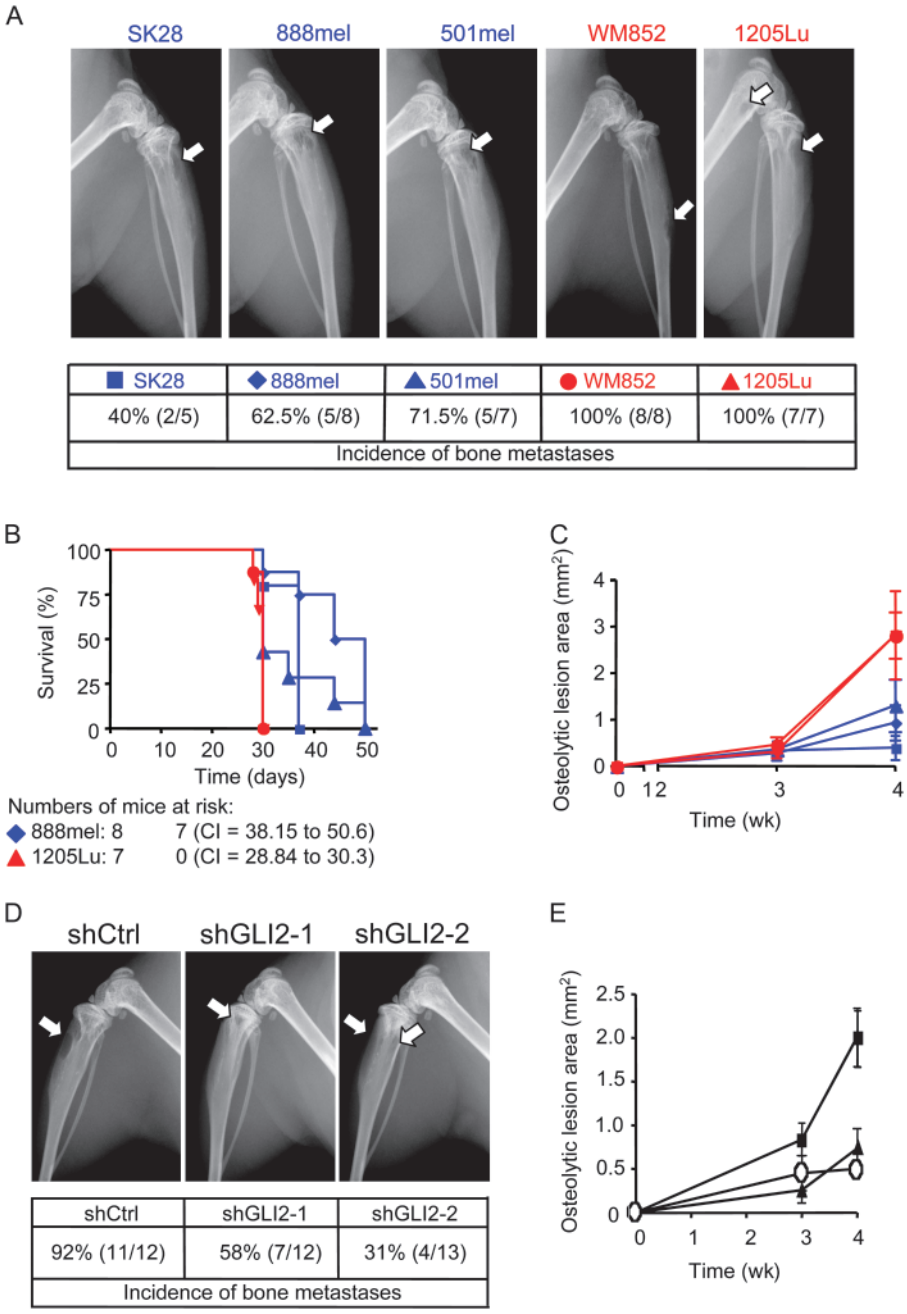

Figure 3. GLI2 expression in melanoma cells and incidence of bone metastasis in mice. **A**) Incidence of bone metastasis. Mice (n = 5–8) were inoculated by injection of the left cardiac ventricle with GLI2high melanoma cells (1205Lu and WM852) or GLI2low cell lines (SK28, 888Mel, and 501Mel). The development of bone metastases is shown by representative x-ray images of the hind limbs of the mice at 4 weeks after intracardiac inoculation. **Arrows** indicate osteolytic lesions. For each cell type, the percent incidence of bone metastases is shown. **B**) Mouse survival. Kaplan–Meier curves are shown for mice inoculated with various melanoma cell lines. Cells expressing high amounts of GLI2 (GLI2high) are shown in **red**, and cells expressing low amounts (GLI2low) are shown in **blue**. **Blue squares**: SK28, **blue diamonds**: 888mel, **blue triangles**: 501mel, **red circles**: WM852, **red triangles**: 1205Lu. The Mann–Whitney test was used to assess the difference in survival between groups. Mice inoculated with GLI2low cells survived longer than those with GLI2 cells (mean survival for all GLI2high cell lines [1205Lu + WM852] = 29.7 days, mean survival for all GLI2low cell lines [888mel + SK28 + 501mel] = 39.1 days, difference = 9.4 days, 95% confidence interval [CI] = 5.22 to 13.64, $P < .001$). The number of mice at risk (for those inoculated with 1205Lu or 888mel melanoma cells) at days 0 and 30 and the 95% confidence interval for survival at 4 weeks are also shown. **C**) Osteolytic lesion area following intracardiac inoculation of melanoma cells in mice. **Blue squares**: SK28, **blue diamonds**: 888mel, **blue triangles**: 501mel, **red circles**: WM852, **red triangles**: 1205Lu. **Error bars** are 95% confidence intervals. Two-way analysis of variance with Bonferroni posttests adjusted for multiple comparisons: 1205 vs SK28: $P < .001$; 1205Lu vs 888mel: $P < .001$; 1205Lu vs 501mel: $P < .01$; 1205Lu vs WM852: not significantly different (n.s.); WM852 vs SK28: $P < .001$; WM852 vs 888mel: $P < .001$; WM852 vs 501mel: $P < .01$; SK28 vs 888mel: n.s., SK28 vs 501mel: n.s., 888mel vs 501mel: n.s. All GLI2high (1205Lu + WM852) vs all GLI2low (SK28 + 888mel + 501mel): $P < .001$. **Error bars** reflect 95% confidence intervals. **D**) Effect of *GLI2* silencing on the incidence of bone metastasis after intracardiac inoculation. Representative x-ray images of the hind limbs of mice (n = 12–13) bearing bone metastases 4 weeks after the inoculation of 1205Lu melanoma cells expressing either of two short hairpin RNAs (shRNAs) to GLI2 (shGLI2-1 and shGLI2-2) vs control shRNA (shCtrl) are shown. **Arrows** indicate osteolytic lesions, and for each cell type, the percent incidence of bone metastases is shown. **E**) Incidence of osteolytic metastases in mice (n = 12–13) following intracardiac injection of 1205Lu cells that expressed GLI2 or control shRNA. The area occupied by osteolytic lesions on radiographs was measured by computerized image analysis of radiographs of the forelimbs and hind limbs at 4 weeks postinoculation. The size of metastases from mice with the following is shown: **black squares**, cells with control shRNA (shCtrl); **black triangles**, shGLI2-1; **open circles**, shGLI2-2 (shCtrl vs shGLI2-1: $P < .05$; shCtrl vs shGLI2-2: $P < .001$). **Error bars** reflect 95% confidence intervals.

501mel], 2.81 vs 0.93 mm², difference = 1.88 mm², 95% CI = 1.16 to 2.60, $P < .001$; mean for 1205Lu vs SK28, 2.82 vs 0.399 mm², difference = 2.42 mm², 95% CI = 0.7 to 4.1, $P < .001$; mean for 1205Lu vs 888mel, 2.82 vs 1.03 mm², difference = 1.88 mm², 95% CI = 0.34 to 3.41, $P < .001$; mean for 1205Lu vs 501mel, 2.82 vs 1.3 mm², difference = 1.51 mm², 95% CI = 0.06 to 3.09, $P = .009$; mean for WM852 vs SK28, 2.81vs 0.39 mm², difference = 2.41 mm², 95% CI = 0.79 to 4.03, $P < .001$; mean for WM852 vs 888mel, 2.81 vs 0.93 mm², respectively, difference = 1.87 mm², 95% CI = 0.45 to 3.29, $P < .001$; mean for WM852 vs 501mel, 2.81 vs 1.3 mm², difference = 1.51 mm², 95% CI = 0.03 to 2.98, $P = .008$). There was no statistical difference between the mean values within each group (GLI2high, 1205Lu vs WM852; GLI2low: SK28 vs 888Mel, SK28 vs 501Mel, 888Mel vs 501Mel) (Figure 3, C). Taken together, these data demonstrate that high GLI2 expression is associated with increased incidence of metastasis, larger osteolytic lesions, and increased morbidity.

To determine whether there is a causal relationship between GLI2 expression and metastasis, two distinct populations of 1205Lu melanoma cells in which GLI2 expression was reduced with shRNA were compared with mock-transduced cells for the development and progression of bone metastases. Bone metastases developed in 11 of the 12 (92%) mice inoculated with control shRNA-expressing 1205Lu cells, whereas only seven of the 12 (58%) mice that received the first population of shGLI2-expressing 1205Lu cells and four of the 13 (31%) mice that received the second population of shGLI2-expressing cells developed bone metastases (Figure 3, D). Osteolytic bone destruction, as measured by quantitative computerized image analysis on radiographs, was markedly less in mice inoculated with two distinct populations of shGLI2-expressing 1205Lu cells than in mice inoculated with control shRNA-transduced 1205Lu tumor cells (mean osteolytic tumor area for shCtrl vs shGLI2-1, 2.0 vs 0.73 mm^2, difference = -1.26 mm^2, 95% CI = -2.07 to -0.45, $P < .001$; mean for shCtrl vs shGLI2-2, 2.0 vs 0.49 mm^2, difference = -1.50 mm^2, 95% CI = -3.22 to -0.2, $P = .042$; mean for shGLI2-1 vs shGLI2-2, 0.73 vs 0.49 mm^2, difference = -0.24 mm^2, 95% CI = -1.99 to -1.5, $P = .27$) (Figure 3, E).

These experiments demonstrate that GLI2high melanoma cells are more prone to form bone metastases than GLI2low cell lines and that reduction of *GLI2* levels in GLI2high cells dramatically alters their ability to form bone metastases. Together, these data provide compelling evidence for a direct role for GLI2 in driving melanoma metastasis to bone.

GLI2 Expression and Mesenchymal Transition in Melanoma Cells

Changes in cell–cell adhesion molecules are associated with the acquisition of aggressive melanoma cell behavior (4,39,40). In normal skin, E-cadherin, encoded by the *CDH1* gene, is expressed in melanocytes and keratinocytes and causes melanocytes to associate with keratinocytes. As melanoma progresses from its radial growth phase to a vertical growth phase, E-cadherin expression is lost and N-cadherin becomes expressed (4,39,40). N-cadherin, encoded by *CDH2*, allows melanocytes to interact with other N-cadherin–expressing cells, such as dermal fibroblasts and the vascular endothelium, thereby increasing their motility and invasiveness (4,39,40). In turn, these modifications of cell–cell interactions favor metastatic spreading of melanoma. Similar molecular changes occur during carcinoma progression in a cellular process often referred to as epithelial to mesenchymal transition (EMT) (41,42).

Among the transcription factors that are known to inhibit CDH1 expression during EMT are SNAIL and the closely related SLUG, as well as TWIST and SIP1 (42). Therefore, we examined the expression of these genes in our panel of melanoma cell lines by semiquantitative RT-PCR. CDH1 expression was extremely variable (Figure 4, A). However, CDH1 expression levels were independent from those of SNAIL (eg, see lanes 7 and 8 vs 9 and 10). This disparity suggests that elevated SNAIL expression is not sufficient per se to drive the loss of CDH1 expression. Remarkably, none of the GLI2high cell lines (Dauv1, WM852, WM793, or 1205Lu) expressed detectable levels of CDH1 mRNA (lanes 2, 6, 9, and 10). On the other hand, CDH1 mRNA was abundant in all GLI2low cell lines (lanes 1, 3–5, 7, and 8) and in normal melanocytes (lane 11). CDH2 mRNA was expressed in all cell lines that expressed *GLI2* at either high or intermediate levels (lanes 1, 2, and 5–10) and followed a pattern very similar to that of SNAIL mRNA. By contrast with SNAIL mRNA expression, steady-state levels of SLUG, TWIST, and SIP1 mRNA were roughly identical among all melanoma cell lines.

We also performed western blots on lysates from selected melanoma cell lines to determine whether protein expression would be similar to that of mRNA. Western analysis revealed that E-cadherin protein levels paralleled CDH1 mRNA levels in that only GLI2low cell lines had detectable E-cadherin protein expression (Figure 4, B).

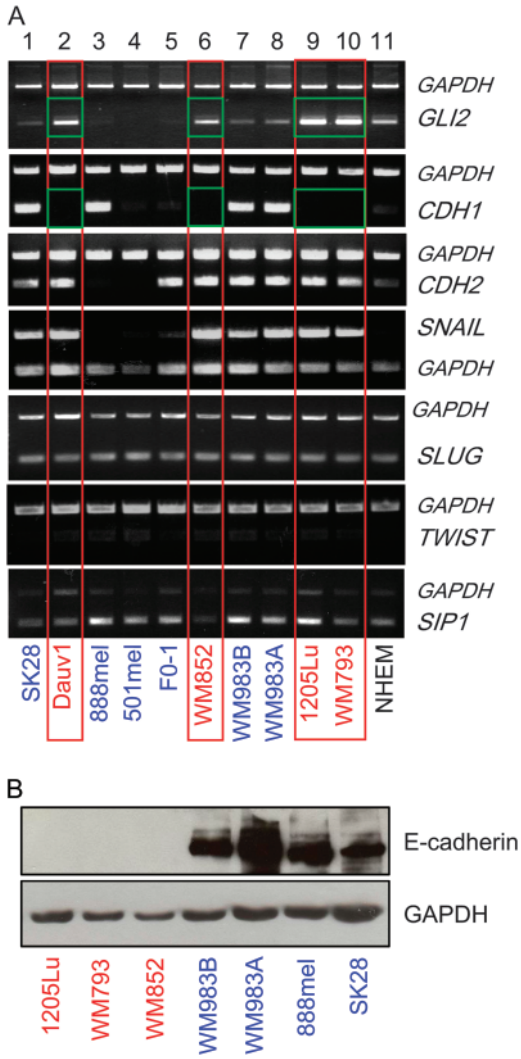

Figure 4. GLI2 expression and loss of E-cadherin in human melanoma cells. **A**) Expression of genes related to epithelial–mesenchymal transition. Total mRNA from four GLI2high human melanoma cell lines (**red**) and six GLI2low melanoma cell lines (**blue**) and from normal human epidermal melanocytes (NHEM cells) was analyzed by multiplex semiquantitative RT-PCR to determine GLI2, CDH1 (E-cadherin), CDH2 (N-cadherin), SNAIL, SLUG, TWIST, and SIP1 expression. Glyceraldehyde-3-phosphate dehydrogenase (*GAPDH*) gene expression was measured simultaneously in each PCR reaction as an internal control. Notable examples of the inverse relationship between GLI2 and CDH1 expression are highlighted in Dauv1, WM852, 1205Lu, and WM793 cell lines (**green frames**). **B**) Western blot analysis of E-cadherin protein levels in melanoma cell lines. E-cadherin was absent in GLI2high cell lines (**red labels**), whereas strong bands were detected in all GLI2low lines (**blue labels**). GLI2 protein levels in the same samples can be found in Figure 1, B.

GLI2 and *CDH1* Expression in Human Cutaneous Melanoma *In Vivo*

We next examined GLI2 and CDH1 expression in three distinct sets of human melanoma samples. First, we performed in situ hybridization to localize areas with high GLI2 mRNA expression in a panel of 20 primary cutaneous melanoma lesions from the Department of Pathology in Nijmegen, the Netherlands. Parallel sections were immunostained for E-cadherin protein localization. We consistently observed heterogeneous expression of GLI2 and CDH1 in all tumor samples (representative examples in Figure 5, A, and in Supplementary Figure 1, available online). Specifically, in situ hybridization of a GLI2 riboprobe revealed strong GLI2 expression in the deep dermal compartment (Figure 5, A, panel e) but not in the superficial compartment (Figure 5, A, panel b) of the skin. In accordance with the expression pattern in melanoma cell lines (see Figure 4), tumor areas with low GLI2 expression were positive for presence of E-cadherin protein, as visualized by immunohistochemistry (Figure 5, A, panels c and d), whereas regions with elevated GLI2 mRNA were E-cadherin negative (Figure 5, A, panels f and g). High power magnification showed that E-cadherin protein expression was localized to the plasma membrane in GLI2-negative tumor cells (Figure 5, A, panel d).

Second, a panel of 17 cutaneous melanoma lymph node metastases from Hôpital Ambroise Paré in Boulogne-Billancourt, France, was screened for the expression of *GLI2* and of *CDH1* by multiplex semiquantitative RT-PCR. Of these 17 samples, two had notably higher levels of GLI2 mRNA (Figure 5, B, lanes 6 and 15, respectively), associated with low expression of CDH1 mRNA. All samples exhibited similar expression levels of the calcium-binding protein *S100A6* gene, a specific marker of neural crest–derived cells that was used to demonstrate the presence of equivalent tumor material in all samples.

Third, GLI2 and CDH1 expression were determined in 42 randomly selected human melanoma samples from the UMDNJ Medical Center that represented four distinct stages of melanoma progression. The lowest levels of GLI2 expression were found in primary melanoma samples, and the highest levels were in distant metastases; however, these differences were not statistically significant (mean GLI2 expression in distant metastases vs primary tumors, 3.21 vs 1.18 relative units normalized against cyclophylin A (*PPIA*) expression, difference = −2.03, 95% CI = −5.29 to 1.23, $P = .27$) (Figure 5, C, left panel). Consistent with our findings in the melanoma cell lines, statistically significantly lower levels of CDH1 mRNA were detected in distant metastases as compared with primary tumors (CDH1 expression in distant metastases vs primary tumors, mean = 31.87 vs 123.6 relative units normalized against cyclophylin A; difference = 91.71, 95% CI = −8.89 to 192.3, $P = .032$) (Figure 5, C, center panel).

Discussion

In this report, we analyzed the specific role played by GLI2 in human melanoma. We demonstrated that GLI2 expression in melanoma cells is highly variable. High GLI2 expression was associated with an invasive and metastatic phenotype in vitro and in vivo and with mesenchymal traits, such as loss of E-cadherin expression and enhanced MMP secretion. Likewise, in human melanoma tumors, increased GLI2 expression was associated with loss of E-cadherin protein expression. Taken together, these data implicate GLI2 as an important modulator of melanoma progression and metastasis.

Over the past several years, major advances have been made in the identification of genetic and environmental factors that contribute to melanoma development. Defining biomarkers that are predictive of the risk of metastasis remains a major challenge. In this report, we demonstrate that GLI2 is a potent modulator of melanoma invasion and metastasis. Its expression is highly variable among human melanoma cell lines and tissue samples and is inversely correlated with the loss of E-cadherin protein expression. In functional studies, we unveil a direct role for GLI2 in driving melanoma cell invasiveness and metastasis. We previously identified GLI2 as a direct target of TGF-β signaling (23). Consistently, we found that high GLI2 expression in aggressive melanoma cell lines is driven, at least in part, by either autocrine or paracrine TGF-β signaling. Exogenous TGF-β is a potent inducer of GLI2 expression in a variety of cell types including melanoma cells (23), irrespective of their basal GLI2 expression status (data not shown). Incubation of the GLI2high cell lines 1205Lu and WM852 with the TGF-β receptor-I kinase inhibitor SB431542 resulted in a three- to fourfold reduction in steady-state levels of GLI2 mRNA (data not shown). We previously demonstrated that either systemic inhibition of TGF-β signaling with the small molecule TGF-β receptor-I inhibitor, SD-208, or overexpression of an inhibitory signaling component, SMAD7, can inhibit melanoma cell invasion in vitro and reduce the occurrence of experimental bone metastases in a mouse model (22,43). In the assays of bone metastasis in mice, both SD-208 and SMAD7 overexpression dramatically reduced GLI2 expression as retrospectively evaluated by real-time RT-PCR (data not shown). Likewise, in breast cancer cells, inhibition of TGF-β signaling also efficiently abrogated bone metastasis (33), whereas overexpression of GLI2 increased bone metastasis (44). Targeting *GLI2* expression in melanoma cells by means of a specific shRNA dramatically reduced invasion of extracellular matrix in vitro (Figure 2) and experimental metastasis to bone in mice (Figure 3), two processes that are highly dependent on TGF-β signaling (21,22). Our findings thus provide new support for a critical role played by GLI2 downstream of TGF-β signaling to drive melanoma metastasis.

In epithelial cancers, loss of E-cadherin protein expression is a hallmark of EMT. This phenomenon is a complex phenotypic conversion that involves changes in morphology, differentiation markers, and cell–cell adhesion molecules, and acquisition of a motile behavior (42) that is functionally associated with poor prognosis in various cancers (41,45,46). Likewise, a mesenchymal transition is characteristic of melanoma switch from an early radial growth phase to vertical growth phase and subsequent metastasis (47,48). In this report, we determined that melanoma cell lines that exhibit high GLI2 at either the mRNA or the protein levels do not express E-cadherin. Reduction of GLI2 protein levels using shRNA provided evidence for a direct role for GLI2 in controlling melanoma invasion and metastasis to bone. We establish that high GLI2 expression in melanoma cell lines is associated with their metastatic potential and inversely correlated with loss of E-cadherin. Our expression data clearly indicate that loss of CDH1 expression is not necessarily associated with changes in SNAIL, SLUG, or TWIST expression, whereas it is consistently associated

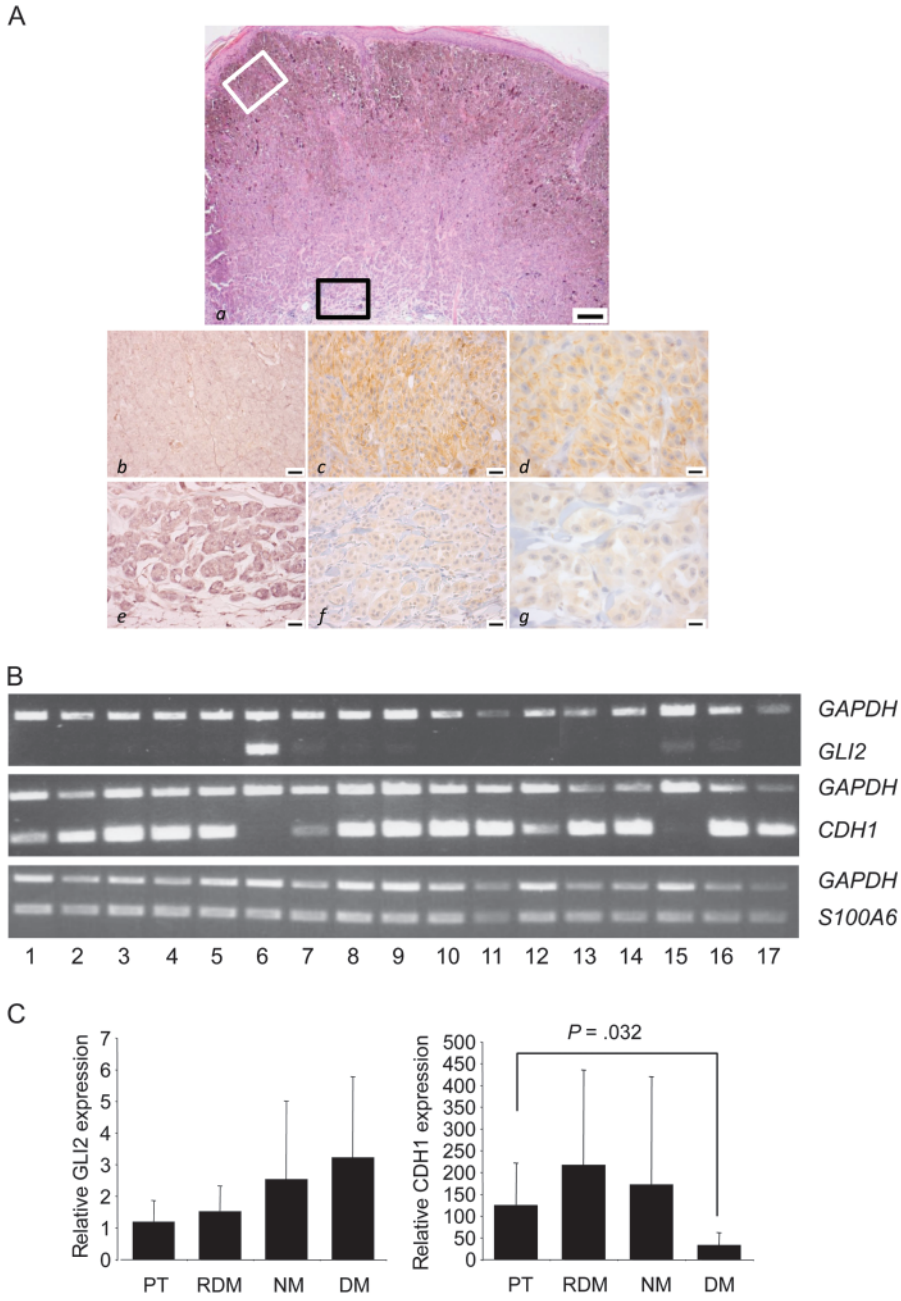

Figure 5. GLI2 expression and loss of E-cadherin in human melanoma lesions. **A**) Variously stained sections of a representative primary cutaneous melanoma are shown. Panel (**a**) shows a hematoxylin and eosin–stained section of the tumor at low magnification (scale bar = 200 μm). Adjacent sections from the superficial (**white box**; panels **b**–**d**) and deep dermal (**black box**; panels **e**–**g**) layers were stained with either a riboprobe to detect GLI2 mRNA (panels **b** and **e**) or a monoclonal antibody to detect E-cadherin protein (panels **c**, **d**, **f**, and **g**) and are shown in more detail (**scale bars** for b, c, e, and f = 25 μm; for d and g = 12.5 μm). Additional photomicrographs of GLI2 and E-cadherin–stained primary melanoma tumor sections can be found in Supplementary Figure 1, available online. **B**) Semiquantitative multiplex reverse transcription–polymerase chain reaction (RT-PCR) to determine GLI2 and CDH1 (E-cadherin) expression levels in total RNA extracted from a panel of 17 frozen human melanoma lymph node metastases. Expression of the *S100A6* calcium-binding protein and *GAPDH* (glyceraldehyde-3-phosphate dehydrogenase) genes was also determined as an internal control. Note the absence of CDH1 mRNA in samples strongly expressing *GLI2*. **C**) Real-time RT-PCR analysis of GLI2 (left panel) and CDH1 (right panel) expression in 42 frozen melanoma samples classified according to tumor stage. DM = distant metastasis; NM = nodal metastasis; PT = primary tumor; RDM = regional dermal metastasis. Values are the mean of 10 samples in each group (12 for the DM group), each of them measured in triplicate and standardized relative to cyclophilin A expression. **Error bars** reflect 95% confidence intervals. *P* value was determined using the Mann–Whitney test. All statistical tests were two-sided.

with elevated steady-state levels of GLI2 mRNA (see Figure 4). Interestingly, the GLI1 protein, a direct GLI2 target (37), was shown to induce EMT in rat kidney epithelial cells via induction of the E-cadherin repressor, SNAIL (49). Future investigations will focus on the molecular events by which GLI2 controls the transition of melanoma cells to a mesenchymal phenotype.

Remarkably, opposite expression of GLI2 and CDH1 was also found in human melanoma samples. Using three independent sets of samples with distinct experimental approaches, we found that melanoma lesions express GLI2 and CDH1 at variable levels and that melanoma lesions are heterogeneous for GLI2 and E-cadherin expression and/or distribution. These findings are consistent with recent reports in the literature that have identified new regulators of melanoma progression, such as Brn2 or Dia-1, whose expression is also heterogeneous within tumors (50,51). E-cadherin plays a critical role in maintaining melanocyte interactions with epidermal keratinocytes and thus keeps progression to a metastatic state at bay. It is therefore reasonable to hypothesize that GLI2 may be a marker of melanoma aggressiveness; first, GLI2high melanoma cell lines are more invasive and metastatic than GLI2low cells, and second, high *GLI2* expression in primary melanoma lesions was localized in the deeper part of the tumors and was consistent with a possible role for GLI2 in the progression toward an invasive phenotype. Larger cohorts of samples will be necessary to validate this observation.

Increased GLI2 expression was accompanied with statistically significant reduction of CDH1 expression in distant metastases as compared with primary melanoma tumors (Figure 5, C). In two sets of samples, we also examined whether more aggressive tumors expressed GLI2 at higher levels than less aggressive ones.

In making this assessment, we used clinical observations of time to metastasis and the extent of initial metastatic spread to define tumor aggressiveness. We found that the two most aggressive primary tumors and the two most aggressive distant metastatic lesions in this study expressed higher levels of GLI2 mRNA compared with their less aggressive counterparts. Inversely, in these two groups, the tumors that expressed the lowest levels of GLI2 mRNA were much more indolent.

This study has several limitations. First, we demonstrated a role for GLI2 in the metastatic activity of melanoma cells in vitro and in a mouse model of bone metastasis in which the experiments were conducted with immunocompromised mice. Immune function may affect the growth and dissemination of melanoma in human patients. In future investigations, it will be important to study whether GLI2 targeting interferes with melanoma metastasis in animal models with spontaneous metastasis. Second, we were not able to measure GLI2 protein levels in human tissue because of the lack of a suitable antibody when these studies were performed, and the number of human specimens that we analyzed was rather small. Newly released commercial antibodies are currently being tested for their specificity. Once adequate antibodies become available, immunohistochemical analyses will be performed on tissues from a larger cohort of patients, with sufficient sample size to allow us to determine whether there is a direct correlation between GLI2 protein expression and histopathological staging of human melanoma.

Taken together, our findings provide a strong rationale to further investigate the role of GLI2 in the initiation and progression of melanoma. Our future goals include the generation of genetic mouse models in which GLI2 function is altered specifically in the melanocyte lineage. It will also be very important to investigate whether GLI2 expression, or the GLI2 to CDH1 ratio, may be a marker of a more aggressive melanoma phenotype in a large cohort of human melanoma samples.

Supplementary Data

Supplementary data can be found at http://www.jnci.oxfordjournals.org/.

References

1. Houghton AN, Polsky D. Focus on melanoma. *Cancer Cell.* 2002;2(4):275–278.
2. Bastian BC. Molecular genetics of melanocytic neoplasia: practical applications for diagnosis. *Pathology.* 2004;36(5):458–461.
3. Curtin JA, Fridlyand J, Kageshita T, et al. Distinct sets of genetic alterations in melanoma. *N Engl J Med.* 2005;353(20):2135–2147.
4. Crowson AN, Magro C, Miller A, Mihm MC Jr. The molecular basis of melanomagenesis and the metastatic phenotype. *Semin Oncol.* 2007;34(6):476–490.
5. Smalley KS. A pivotal role for ERK in the oncogenic behaviour of malignant melanoma? *Int J Cancer.* 2003;104(5):527–532.
6. Chin L, Garraway LA, Fisher DE. Malignant melanoma: genetics and therapeutics in the genomic era. *Genes Dev.* 2006;20(16):2149–2182.
7. Ingham PW, McMahon AP. Hedgehog signaling in animal development: paradigms and principles. *Genes Dev.* 2001;15(23):3059–3087.
8. Varjosalo M, Taipale J. Hedgehog: functions and mechanisms. *Genes Dev.* 2008;22(18):2454–2472.
9. McMahon AP, Ingham PW, Tabin CJ. Developmental roles and clinical significance of hedgehog signaling. *Curr Top Dev Biol.* 2003;53:1–114.
10. Ruiz i Altaba A. Sanchez P, Dahmane N. Gli and hedgehog in cancer: tumours, embryos and stem cells. *Nat Rev Cancer.* 2002;2(5):361–372.
11. Stecca B, Mas C, Clement V, et al. Melanomas require HEDGEHOG-GLI signaling regulated by interactions between GLI1 and the RAS-MEK/AKT pathways. *Proc Natl Acad Sci U S A.* 2007;104(14):5895–5900.
12. Derynck R, Akhurst RJ, Balmain A. TGF-beta signaling in tumor suppression and cancer progression. *Nat Genet.* 2001;29(2):117–129.
13. Javelaud D, Mauviel A. Mammalian transforming growth factor-betas: Smad signaling and physio-pathological roles. *Int J Biochem Cell Biol.* 2004;36(7):1161–1165.
14. Massague J. TGFbeta in Cancer. *Cell.* 2008;134(2):215–230.
15. Massague J, Seoane J, Wotton D. Smad transcription factors. *Genes Dev.* 2005;19(23):2783–2810.
16. Feng XH, Derynck R. Specificity and versatility in tgf-beta signaling through Smads. *Annu Rev Cell Dev Biol.* 2005;21:659–693.
17. Van Belle P, Rodeck U, Nuamah I, Halpern AC, Elder DE. Melanoma-associated expression of transforming growth factor-beta isoforms. *Am J Pathol.* 1996;148(6):1887–1894.
18. Krasagakis K, Tholke D, Farthmann B, Eberle J, Mansmann U, Orfanos CE. Elevated plasma levels of transforming growth factor (TGF)-beta1 and TGF-beta2 in patients with disseminated malignant melanoma. *Br J Cancer.* 1998;77(9):1492–1494.
19. Javelaud D, Alexaki VI, Mauviel A. Transforming growth factor-beta in cutaneous melanoma. *Pigment Cell Melanoma Res.* 2008;21(2):123–132.
20. Rodeck U, Nishiyama T, Mauviel A. Independent regulation of growth and SMAD-mediated transcription by transforming growth factor beta in human melanoma cells. *Cancer Res.* 1999;59(3):547–550.
21. Javelaud D, Delmas V, Moller M, et al. Stable overexpression of Smad7 in human melanoma cells inhibits their tumorigenicity in vitro and in vivo. *Oncogene.* 2005;24(51):7624–7629.
22. Javelaud D, Mohammad KS, McKenna CR, et al. Stable overexpression of Smad7 in human melanoma cells impairs bone metastasis. *Cancer Res.* 2007;67(5):2317–2324.
23. Dennler S, Andre J, Alexaki I, et al. Induction of sonic hedgehog mediators by transforming growth factor-beta: Smad3-dependent activation of Gli2 and Gli1 expression in vitro and in vivo. *Cancer Res.* 2007;67(14):6981–6986.
24. Dumaz N, Hayward R, Martin J, et al. In melanoma, RAS mutations are accompanied by switching signaling from BRAF to CRAF and disrupted cyclic AMP signaling. *Cancer Res.* 2006;66(19):9483–9491.
25. Rodeck U, Melber K, Kath R, et al. Constitutive expression of multiple growth factor genes by melanoma cells but not normal melanocytes. *J Invest Dermatol.* 1991;97(1):20–26.
26. MacDougall JR, Kobayashi H, Kerbel RS. Responsiveness of normal, dysplastic melanocytes and melanoma cells from different lesional stages of disease progression to the growth inhibitory effects of TGF-beta. *Mol Cell Diff.* 1993;1:21–40.
27. Moore R, Champeval D, Denat L, et al. Involvement of cadherins 7 and 20 in mouse embryogenesis and melanocyte transformation. *Oncogene.* 2004;23(40):6726–6735.
28. Sasaki H, Hui C, Nakafuku M, Kondoh H. A binding site for Gli proteins is essential for HNF-3beta floor plate enhancer activity in transgenics and can respond to Shh in vitro. *Development.* 1997;124(7):1313–1322.
29. Sasaki H, Nishizaki Y, Hui C, Nakafuku M, Kondoh H. Regulation of Gli2 and Gli3 activities by an amino-terminal repression domain: implication of Gli2 and Gli3 as primary mediators of Shh signaling. *Development.* 1999;126(17):3915–3924.
30. Overall CM, Wrana JL, Sodek J. Independent regulation of collagenase, 72-kDa progelatinase, and metalloendoproteinase inhibitor expression in human fibroblasts by transforming growth factor-beta. *J Biol Chem.* 1989;264(3):1860–1869.
31. Guise TA, Yin JJ, Taylor SD, et al. Evidence for a causal role of parathyroid hormone-related protein in the pathogenesis of human breast cancer-mediated osteolysis. *J Clin Invest.* 1996;98(7):1544–1549.
32. Kang Y, Siegel PM, Shu W, et al. A multigenic program mediating breast cancer metastasis to bone. *Cancer Cell.* 2003;3(6):537–549.
33. Yin JJ, Selander K, Chirgwin JM, et al. TGF-beta signaling blockade inhibits PTHrP secretion by breast cancer cells and bone metastases development. *J Clin Invest.* 1999;103(2):197–206.

34. van Kempen LC, Rijntjes J, Claes A, et al. Type I collagen synthesis parallels the conversion of keratinocytic intraepidermal neoplasia to cutaneous squamous cell carcinoma. *J Pathol.* 2004;204(3):333–339.
35. Goydos JS, Gorski DH. Vascular endothelial growth factor C mRNA expression correlates with stage of progression in patients with melanoma. *Clin Cancer Res.* 2003;9(16, pt 1):5962–5967.
36. Agren M, Kogerman P, Kleman MI, Wessling M, Toftgard R. Expression of the PTCH1 tumor suppressor gene is regulated by alternative promoters and a single functional Gli-binding site. *Gene.* 2004;330:101–114.
37. Ikram MS, Neill GW, Regl G, et al. GLI2 is expressed in normal human epidermis and BCC and induces GLI1 expression by binding to its promoter. *J Invest Dermatol.* 2004;122(6):1503–1509.
38. Deryugina EI, Quigley JP. Matrix metalloproteinases and tumor metastasis. *Cancer Metastasis Rev.* 2006;25(1):9–34.
39. Nesbit M, Herlyn M. Adhesion receptors in human melanoma progression. *Invasion Metastasis.* 1994;14(1–6):131–146.
40. Miller AJ, Mihm MC Jr. *Melanoma. N Engl J Med.* 2006;355(1):51–65.
41. Guarino M, Rubino B, Ballabio G. The role of epithelial-mesenchymal transition in cancer pathology. *Pathology.* 2007;39(3):305–318.
42. Huber MA, Kraut N, Beug H. Molecular requirements for epithelial-mesenchymal transition during tumor progression. *Curr Opin Cell Biol.* 2005;17(5):548–558.
43. Mauviel A, Javelaud D, Mohammad KS, Guise TA. The transforming growth factor beta receptor I kinase inhibitor SD-208 reduces the development and progression of melanoma bone metastasis. *J Invest Dermatol.* 2007;127(suppl 2):S48.
44. Sterling JA, Oyajobi BO, Grubbs B, et al. The hedgehog signaling molecule Gli2 induces parathyroid hormone-related peptide expression and osteolysis in metastatic human breast cancer cells. *Cancer Res.* 2006; 66(15):7548–7553.
45. Vincent-Salomon A, Thiery JP. Host microenvironment in breast cancer development: epithelial-mesenchymal transition in breast cancer development. *Breast Cancer Res.* 2003;5(2):101–106.
46. Yang J, Weinberg RA. Epithelial-mesenchymal transition: at the crossroads of development and tumor metastasis. *Dev Cell.* 2008;14(6):818–829.
47. Gruss C, Herlyn M. Role of cadherins and matrixins in melanoma. *Curr Opin Oncol.* 2001;13(2):117–123.
48. Bonitsis N, Batistatou A, Karantima S, Charalabopoulos K. The role of cadherin/catenin complex in malignant melanoma. *Exp Oncol.* 2006;28(3): 187–193.
49. Li X, Deng W, Nail CD, et al. Snail induction is an early response to Gli1 that determines the efficiency of epithelial transformation. *Oncogene.* 2006; 25(4):609–621.
50. Carreira S, Goodall J, Denat L, et al. Mitf regulation of Dia1 controls melanoma proliferation and invasiveness. *Genes Dev.* 2006;20(24):3426–3439.
51. Goodall J, Carreira S, Denat L, et al. Brn-2 represses microphthalmia-associated transcription factor expression and marks a distinct subpopulation of microphthalmia-associated transcription factor-negative melanoma cells. *Cancer Res.* 2008;68(19):7788–7794.

Funding

This work was supported by grants from INSERM, INCa PLBIO08-126, Cancéropole Ile-de-France RS-013, Ligue Nationale Contre le Cancer/Comité des Yvelines, and by a donation from Emile and Henriette Goutière to A. M., and by an National Institutes of Health RO1 grant (CA69158) to T.A.G.

Notes

V.-I. Alexaki and D. Javelaud have contributed equally to the work.

The sponsors of this study had no role in the collection of the data, the analysis and interpretation of the data, the decision to submit the manuscript for publication, or the writing or the manuscript.

We thank Martin F. M. de Rooij (Department of Pathology, Radboud University Nijmegen Medical Centre) for technical assistance.

Affiliations of authors: INSERM U697, Paris, France (V-IA, DJ, SD, FV, AM); Institut Curie, Centre de Recherche, Orsay, France (DJ, SD, FL, SS, VD, LL, AM); INSERM U1021, Orsay, France (DJ, SD, FL, SS, VD, LL, AM); CNRS UMR3347, Orsay, France (DJ, SD, FL, SS, VD, LL, AM); Université Paris XI, Orsay, France (DJ, SD, FL, SS, VD, LL, AM); Department of Pathology, Radboud University Nijmegen Medical Centre, Nijmegen, the Netherlands (LCLVK); Division of Endocrinology, Department of Medicine, Indiana University, IUPUI, Indianapolis, IN (KSM, PJ, PJF, TAG); Department of Dermatology, University Hospital of Zurich, Zurich, Switzerland (KH); Department of Surgery, University of Medicine and Dentistry of New Jersey, Robert Wood Johnson Medical School, New Brunswick, NJ (JSG); Service de Dermatologie, Hôpital Ambroise Paré, Boulogne, France (CS, PS); INSERM U895, Nice, France (CB, RB).